Regulation of Canonical NF-κB Signaling in Macrophages by *Cryptococcus neoformans* Capsular Polysaccharide

by
Lauren Heusinkveld

A thesis presented to the Honors College of Middle Tennessee State University in partial fulfillment of the requirements for graduation from the University Honors College

Fall 2015

Acknowledgements

I would like to thank Drs. David Nelson and Erin McClelland for their invaluable mentorship and unfailing support during this laboratory research project. I would also like to thank James Hayes, Dr. Kevin Bicker, and Larissa Wolf for their assistance with developing methodologies. This project was supported by two URECA Silver Scholar Grants (Undergraduate Research Center, MTSU) and a Grant-In-Aid of Research (Sigma Xi Scientific Research Society).

Abstract

Cryptococcus neoformans (*Cn*) is a ubiquitous fungal pathogen that causes meningitis in immunocompromised individuals. The major virulence factor of *Cn* is a thick polysaccharide capsule composed of glucuronoxylomannan (GXM) and galactoxylomannan (GalXM). GXM has been implicated in altering NF-κB signaling in macrophages, which constitute one of the first defenses against *Cn* infection. Capsular polysaccharides were isolated from Serotype A *Cn*, wildtype strain H99S, GalXM-negative Uge1, and GXM-negative Cap59. RAW 264.7 NF-κB reporter cells with p65 expressed as a chimeric fusion protein with GFP (p65-EGFP) were treated with GXM and LPS or LPS alone and imaged via live single cell microscopy. GXM treatment was associated with profound suppression of p65 nuclear translocation. Coupled with studies involving whole *Cn* using this model of macrophage *Cn* infection, the results of this project will yield valuable insights into the mechanisms by which *Cn* subverts the host immune response.

Table of Contents

Tables

Figures

Abbreviations

Abbreviations follow standard SI conventions for units with the following additions:
AIDS – acquired immunodeficiency syndrome
Akt – protein kinase B
ANOVA – analysis of variance
AP – alkaline phosphatase
ATP – adenosine triphosphate
BSA – bovine serum albumin
Cn – *Cryptococcus neoformans*
CNS – central nervous system
CTAB – cetyltriammonium bromide
diH_2O – deionized water
DMEM – Dubecco's modified eagle medium
DTT – dithiothreitol
EDTA - ethylenediaminetetraacetic acid
ELISA – enzyme-linked immunosorbent assay
ETF – endotoxin-free
EU – endotoxin units
FBS – fetal bovine serum
FcγRIIb - fragment crystallizable gamma receptor IIb
GalXM – galactoxylomannan
GFP – green fluorescent protein
GXM – glucuronoxylomannan
IFNγ – interferon-gamma
iNOS – inducible nitric oxide synthase
IKK – IκB kinase
IL – interleukin
LAL – limulus amebocyte lysate
LPS – lipopolysaccharide
mAb – monoclonal antibody
MyD88 – myeloid differentiation primary response 88
NF-κB – nuclear factor kappa-light-chain-enhancer of activated B cells
PBS – phosphate-buffered saline
PMB – Polymyxin B
PMSF – phenylmethanesulfonyl fluoride
PNPP – p-nitrophenyl phosphate
RLU – relative light units
ROI – region of interest
SHIP – SH2-containing inositol phosphatase
TB – Trypan blue
TBS/T – tris-buffered saline/tween 20
TLR – toll-like receptor
TNFα – tumor necrosis factor-alpha
YPD – yeast peptone dextrose

1

INTRODUCTION

1.1 Background

Cryptococcus neoformans (*Cn*) is an opportunistic fungal yeast that causes life-threatening cryptococcal meningitis in individuals with compromised immune function, particularly AIDS patients[1]. *Cn* is prevalent worldwide and commonly found in the soil and in bird guano[1]. The respiratory system is the most common point of entry for *Cn* spores. In immunocompetent people, spores typically enter a latent state and remain in the lungs[2]. However, disseminated cryptococcal infection may result in meningitis associated with central nervous system (CNS) invasion[3]. Thus decreased immune function or a new infection in an immunocompromised patient can lead to fatal neurological damage by *Cn*. *Cn*'s major virulence factor is a thick polysaccharide capsule[4] (Figure 1), which is an unusual trait in fungi that act as human pathogens[5]. The capsule is composed primarily of two polysaccharides, glucuronoxylomannan (GXM; ~90%) and galactoxylomannan (GalXM; 5-8%)[6], which are shed during replication. GXM is detectable in the μg/mL range in blood serum and cerebrospinal fluid of infected patients[7,8,9].

While the threat to human health posed by *Cn* has increased substantially in the last few decades, we have been aware of *Cn* for over a century. *Cn* was first described by European scientists in the mid-1890s[10,11]. Sanfelice[10,12] isolated *Cn* from a sample of peach juice, and Busse[10,13] and Buschke[10,14] discovered the pathogen in a patient's tibial lesion. Von Hansemann was the first to report cryptococcal meningitis in 1905[10,15]. Increasing recognition of cryptococcoal infection by physicians, medical advances in

immunosuppressive therapies, and the advent of the AIDS pandemic contributed to a dramatic rise in the importance of *Cn* from a public health perspective throughout the twentieth century[16]. Currently *Cn* is considered an AIDS-defining pathogen[1,11]. It is the leading cause of fungal infection[1,10,11] and the third most common cause of neurological complications[11] in AIDS patients.

Alveolar macrophage immune cells constitute one of the first lines of defense against *Cn* infections[17]. Macrophages engulf pathogens such as *Cn* by a process called phagocytosis, reviewed by Coelho *et al*[17], and also ingest free cryptococcal polysaccharides[18]. Macrophages alert other immune cells to the onset of an infection by releasing small signaling proteins called cytokines. Tumor necrosis factor-alpha (TNFα) is considered a prototypical cytokine[19], and it is critical in mounting the inflammatory immune response to infection[20].

Cn has evolved multiple mechanisms for evading the immune response, making it versatile and adaptable. Although phagocytosis by macrophages normally serves to destroy pathogens, the fungus thrives intracellularly and may also survive in the extracellular environment within its host[21]. *Cn* can continue to replicate after macrophage phagocytosis, and both whole *Cn*[22] and capsular polysaccharide[23] may remain within macrophages for months. Additionally, Alvarez & Casadevall[24] demonstrated *Cn* is capable of exiting the macrophage by 'phagosomal extrusion' without destroying it. This escape mechanism may have evolved in response to selective pressure from environmental predators such as amoeba. *Cn* typically divides by simply budding but may also reproduce sexually[16]. *Cn* is generally not directly recognized by macrophages; it must be coated or 'opsoninzed' by specific antibodies produced as part of the host's

adaptive immune response or by the complement component C3b before phagocytosis can occur, which causes a delay between infection and phagocytosis[16].

Cn disrupts several macrophage cell-signaling pathways, including nuclear factor kappa-light-chain-enhancer of activated B cells (NF-κB)[21,26,27], compromising their ability to destroy phagocytosed *Cn*. NF-κB describes a family of ubiquitous transcription factors involved in multiple cellular processes including cell cycle, cytokine production, immune system development, and apoptosis[28]. NF-κB transcription factors can be separated into two parallel pathways, canonical and non-canonical, dominated by the activities of either p65- or RelB-containing dimers, respectively. Although these two pathways are intimately related, p65 and RelB have differing affinities for the various transcription targets they regulate. For example, p65 appears to play a greater role in the inflammatory response than RelB.

The canonical pathway can be triggered by a broad range of stimuli, from cytokines to cellular stress and DNA damage, which all promote activation of the IκB kinase (IKK) signalosome[29,30]. This multi-subunit protein complex directs the simultaneous phosphorylation of p65 and its inhibitor, IκBα, stimulating IκBα degradation and concomitant nuclear translocation of p65, where it is able to regulate immediate immune and inflammatory response genes[28]. On the other hand, the non-canonical pathway is activated when the RelB binding partner, p100, is phosphorylated and cleaved by the proteasomes to p52[28]. The non-canonical pathway stimulates B cell maturation and normal T cell function[28]. Therefore, modulation of either or both wings of the NF-κB pathway by *Cn* may compromise the host immune response, weakening an individual's ability to overcome the infection.

Currently available therapies are not sufficient for treating disseminated cryptococcal infections. Only four clinically proven drugs are recommended by the Infectious Diseases Society of America[31]: Amphotericin B, flucytosine, fluconazole, and itraconazole, and these are frequently associated with side effects such as nausea, vomiting, and fever. Hepatic or renal toxicity is also possible[3,32]. Additionally, Amphotericin B is only available intravenously, which limits its utility in developing countries where cryptococcal meningitis is most prevalent[32]. Although isolated pulmonary infections in immunocompetent hosts are often asymptomatic and self-limiting, all symptomatic infections require intensive antifungal regimens[3]. Immunocompromised patients require aggressive treatment for up to twelve months, and lifelong maintenance therapy is necessary to prevent relapse in patients in the later stages of AIDS[31]. A paucity of treatment options combined with long-term fluconazole use increases the threat posed by development of drug resistance in *Cn*[33,34]. Thus, current drugs for combatting cryptococcal infections are limited by severe side effects, lack of access in resource-poor areas, low rates of infection clearance in immunocompromised patients, and increasing antifungal resistance.

New insights into the mechanisms by which *Cn* interacts with host macrophages could provide direction for development of novel treatments. In this undergraduate thesis project, the dynamics of macrophage canonical NF-κB signaling in response to GXM were investigated using a novel live cell fluorescence microscopy approach.

1.2 Rationale

GXM is known to induce dysregulation of NF-κB-mediated proinflammatory pathways in macrophages[26,27,35], and the macrophage receptors toll-like receptor (TLR) 4[26] and

fragment crystallizable gamma receptor IIb (FcγRIIb)[36,37] recognize GXM (Figure 2). GXM appears to both inhibit and partially activate NF-κB signaling by engaging these receptors. TLR4 is the primary receptor for bacterial lipopolysaccharide (LPS), a potent activator of NF-κB[38]. LPS binding recruits myeloid differentiation primary response 88 (MyD88) adaptor proteins to the intracellular TLR4 domains, which then activate protein kinase B (Akt), leading to phosphorylation and degradation of IκBα and release of p65 to the nucleus[37]. TLR4 also recognizes GXM, and Shoham *et al*[26] demonstrated GXM-dependent TLR4 signaling results in NF-κB nuclear translocation without proinflammatory downstream effects such as TNFα expression.

Other investigations have demonstrated a suppressive effect of GXM on proinflammatory NF-κB signaling. Monari *et al*[39] found that GXM significantly reduced LPS-induced TNFα expression without inducing NF-κB signaling through TLR4 in primary macrophages. In a mouse model of LPS-induced endotoxic shock, production of TNFα and interleukin (IL)-6 (also a pro-inflammatory cytokine regulated by NF-κB) was reduced in the lymph nodes and spleens of mice treated with GXM in addition to LPS compared to mice given LPS alone[37]. In addition, IκBα phosphorylation and TNFα production were reduced in RAW 264.7 murine macrophage cells treated with GXM and LPS as opposed to LPS alone. This study also suggested GXM exerts its suppressive effects through FcγRIIb. Upon FcγRIIb binding, SH2-containing inositol phosphatase (SHIP) proteins are activated by phosphorylation and proceed to inhibit MyD88 and Akt, which are involved in TLR4-directed proinflammatory NF-κB signaling (Figure 2). In this manner, GXM suppresses the phosphorylation and degradation of IκBα. Thus, the conflicting reports of GXM's effects on NF-κB activity warrant further investigation.

The previously described research addressing the effects of GXM on NF-κB signaling has overwhelmingly relied upon endpoint assays such as Western blot[37,39], enzyme-linked immunosorbent assay (ELISA)[37], and nuclear fractionation analysis[26]. While informative, such techniques are only able to capture the average behavior of cells. In this project, imaging of individual live cells via fluorescence microscopy was performed to investigate NF-κB signaling activity at high temporal resolution, which could not be achieved by traditional endpoint assays. This novel approach to investigating NF-κB-mediated activity in response to GXM allowed observation of subtle changes in the dynamics of NF-κB signaling that could not otherwise be scrutinized.

2

MATERIALS AND METHODS

2.1 Cryptococcal polysaccharide purification

The initial phase of this project required purification of GXM and GalXM from *Cn* culture supernatant. Three strains of Serotype A *Cn* were used: wildtype H99S, GXM-negative Cap59, and GalXM-negative Uge1. Polysaccharides were purified by both chemical precipitation and ultrafiltration.

2.1.1 Ultrafiltration: GalXM

Isolation of GalXM from Cap59 was attempted using a stirred ultrafiltration cell (EMD Millipore, Billerica, MA; Figure 4). Cap59 was cultured from frozen stock in 50 mL of yeast peptone dextrose (YPD; 10 g yeast extract, 20 g bacto peptone, 20 g dextrose per liter; Becton Dickinson and Company, Franklin Lakes, NJ) at 30°C with shaking at 150 rpm for 3 days. The cells were centrifuged in a Thermo Scientific Legend XTR 7500 centrifuge with a TX-750 rotor (Waltham, MA) at 872 × *g* (2000 rpm) for 5 minutes. The supernatant was discarded and the cells were washed with 15 mL of phosphate-buffered saline (PBS; Mediatech, Inc., Manassas, VA). The cells were then incubated in 200 mL of minimal media (15 mM glucose, 10 mM $MgSO_4$-$7H_2O$, 29.4 mM KH_2PO_4, 0.13 mM glycine, 3 μM thiamine HCl; pH = 6.0) with 1% Penicillin-Streptomycin antibiotics (Sigma Aldrich, St. Louis, MO) under the conditions previously described for 5 days. Cells were centrifuged at 4000 × *g* (4283 rpm) and at 11,000 × *g* (8000 rpm) for 15 minutes. The supernatant containing GalXM was collected and concentration was attempted using a stirred ultrafiltration cell with nitrogen gas. However, the supernatant

passed through the cell too quickly for polysaccharide to accumulate on a 10 kDa filtration membrane, which was the most selective membrane available with respect to size in the McClelland lab. This may be because GalXM is too small to self-aggregate.

2.1.2 Chemical precipitation: GXM + GalXM

GXM and GalXM were purified from wildtype H99S, GXM-negative Cap59, and GalXM-negative Uge1 with 0.2M NaCl and 0.05% cetyltriammonium bromide (CTAB) precipitation as described by Cherniak *et al*[40] followed by additional washing steps with 2% acetate in ethanol, 90% ethanol, and absolute ethanol[41]. H99S, Cap59, and Uge1 were cultured from frozen stock in 50 mL of YPD at 30°C with shaking at 150 rpm until growth reached log phase (1-3 days) and then in 200 mL defined minimal media under the same incubation conditions for 5 days. Yeast cells were centrifuged using a JA-10 rotor in an ultracentrifuge (Beckman Coulter Inc., Pasadena, CA) at 11,000 × *g* (8000 rpm) for 20 minutes. The supernatants were then collected and filter sterilized using a 0.2-micron syringe filter into a protein spin column (10,000 mw/10 kDa cutoff) to concentrate the supernatant. The protein spin column was centrifuged at 4000 × *g* (4283 rpm) with the TX-750 rotor at 4°C until 200 mL of supernatant was concentrated to 8 mL per culture. The concentrates were dialyzed against deionized water for 48 hours to remove any remaining salts from the minimal media, and the polysaccharides were precipitated overnight at -20°C in 3 volumes of absolute ethanol, which was removed using vacuum concentration.

Purification proceeded using 0.2M NaCl and 0.05% CTAB precipitation followed by washing steps to reduce the tonicity of GXM and GalXM samples (Figure 3). The addition of CTAB and NaCl precipitated GXM from GalXM in H99S supernatant. The

GXM pellet was then dried using vacuum concentration and resuspended in LPS-free PBS. The supernatants containing GalXM were dialyzed against milliQ water overnight at 4°C. The dialyzed sample was dried by vacuum concentration. GXM and GalXM samples were dialyzed against deionized water (diH_2O) overnight, precipitated in 3 volumes of absolute ethanol overnight at -80°C, and then washed with 2% acetic acid in ethanol, 90% ethanol, and absolute ethanol. The solutions were centrifuged at 11,000 × *g* (8000 rpm) for 10 minutes followed by vacuum evaporation to remove the supernatant. The remaining pellets were dried using vacuum concentration. To further reduce the tonicity of the samples, GXM and GalXM preps were again dialyzed overnight against diH_2O, precipitated in three volumes of absolute ethanol overnight at -80°C, and the washing steps were repeated. The remaining pellets were dried and resuspended in endotoxin-free (ETF) water (Life Technologies, Carlsbad, CA).

2.1.3 Ultrafiltration: GXM

GXM was isolated from Uge1 culture supernatant by ultrafiltration using methods adapted from Nimrichter *et al*[42]. In brief, Uge1 was cultured in 50 mL of YPD overnight and then in 1.6 L of defined minimal media for 4 days. The cells were centrifuged at 4415 × *g* (4500 rpm) for 10 minutes and at 11,000 × *g* (8000 rpm) for 10 minutes. The supernatant was collected and concentrated using a stirred ultrafiltration cell (Figure 4). Supernatant was pressed through a 50 kDa filtration membrane by nitrogen gas (45-60 psi). The resulting jelly was lyophilized (freeze-dried) and washed with 2% acetic acid in ethanol, 90% ethanol, and absolute ethanol. The solution was centrifuged at 11,000 × *g* (8000 rpm) for 10 minutes followed by vacuum evaporation to remove the supernatant. The remaining GXM pellet was dried and resuspended in ETF water.

2.1.4 Decontamination of polysaccharide preps

LPS was removed from all Uge1-derived GXM samples using a Polymyxin B (PMB) column in ETF water. Polymyxin B is a nonapeptide antibiotic that neutralizes LPS by covalently binding it[43]. To make a PMB column, a disposable column (Thermo Scientific) was filled with ETF water, and a filter was placed in the bottom of the column. Five mL agarose beads linked to PMB (Sigma Aldrich) was added and allowed to settle overnight at 4°C. A second filter was placed on top of the beads. The column was washed 5x with ETF water. Polysaccharide samples were added to the column 5 mL at a time with 12 mL of ETF water. Between each GXM addition, the column was washed with 25 mL of 1% sodium deoxycholate and 25 mL of ETF water to remove LPS, thereby regenerating the column. The samples were then lyophilized, weighed, and re-suspended in ETF water.

2.1.5 GXM validation

2.1.5.1 ELISA

Polysaccharides in our samples were verified and quantified by ELISA with IgG_1 monoclonal antibody (mAb) 18b7, which binds GXM[44] (Figure 5). A 96-well plate was coated with unlabeled goat α-mouse IgM (1:1000; SouthernBiotech, Birmingham, AL) and incubated at 37°C for 1 hour. The plate was blocked with 200 µL/well 1% bovine serum albumin (BSA; Fisher Scientific, Waltham, MA) overnight at 4°C. The plate was then washed three times with tris-buffered saline/tween 20 (TBS/T; 2 M tris pH 7.2, 5 M NaCl, 1 M NaN_3, 1% tween 20). Next, 50 µL/well 2D10[45] (2 µg/mL; courtesy of Dr. Arturo Casadevall, Albert Einstein College of Medicine) was added to the plate to serve as an intermediate between unlabeled IgM and GXM. Following incubation at 37°C for 1

hour, 75 μL of sample (H99S GXM, H99S GXM + GalXM, Uge1 GXM, or GXM standard; 10 μg/mL) was added to the first column and diluted 1:3 down the plate with 1% BSA in PBS. The incubation and TBS/T washes were repeated. The plate was then incubated under the same conditions with 50 μL/well 18b7 mAb (10 μg/mL; courtesy of Dr. Casadevall). The TBS/T washes were repeated. Next the plate was incubated with alkaline phosphatase (AP)-labeled goat anti-mouse IgG_1 (SouthernBiotech) diluted 1:1000 at 37 °C for 1 hour. P-nitrophenyl phosphate (PNPP; Sigma Aldrich), an AP substrate that is converted to a yellow product, was added. After incubation in the dark for 10-15 minutes, absorbance was read at 405 nm using a SpectraMax M5 microplate reader (Molecular Devices, Sunnyvale, CA).

2.1.5.2 Calorimetric sugar assay

A calorimetric sugar assay employing H_2SO_4 and phenol was used to verify and quantify Uge1-derived GXM isolated by chemical precipitation[46]. Two mL of MilliQ water followed by 50 μL of phenol was added to each of nine 50 mL conicals. To make the standards, 2, 5, 15, 20, or 25 μL 1% glucose was added to 6 conicals. Ten μL of Uge1-derived GXM was added to one conical. The remaining conical served as a blank with no glucose or GXM added. Next, 5 mL H_2SO_4 was added to each tube, which caused a highly exothermic reaction resulting in an orange product. After allowing the tubes to cool, the absorbance was read at 485 nm using the SpectraMax M5 microplate reader.

2.1.5.3 Limulus Amebocyte Lysate (LAL) assay

H99S- and Uge1-derived GXM samples were tested for the presence of LPS using a Pierce® LAL Chromogenic Endotoxin Quantitation Kit (Thermo Scientific). All reagents were equilibrated to room temperature before the endotoxin standard stock solutions were

prepared. ETF water (1 mL) was added to lyophilized endotoxin to make the endotoxin standard stock (ESS; 28 EU/mL), which was agitated using a vortex for several minutes. EU stands for endotoxin unit, which is a measure of endotoxin activity. Four stock solutions were prepared: A (1 EU/mL), B (0.5 EU/mL), C (0.25 EU/mL), and D (0.1 EU/mL). All stock solutions were then agitated for 1 minute. Lyophilized limulus amebocyte lysate (LAL) was reconstituted with 1400 µL ETF water. ETF water (6.5 mL) was added to the lyophilized chromogenic substrate. A microplate was equilibrated to 37°C on a heating block for 10 minutes. Standards and unknown samples were added to the plate (50 µL/well), and the plate was incubated at 37°C for 5 minutes. Next, 50 µL of LAL was added to each well. The plate was briefly placed on a plate shaker followed by incubation at 37°C for 10 minutes, and 100 µL of substrate was added to each well. The plate was briefly placed on a plate shaker and then incubated again at 37°C for six minutes. Finally, 50 µL of 25% acetic acid (stop reagent) was added to each well, and the absorbance was read at 405 nm.

2.2 Live cell fluorescence microscopy experiments

2.2.1 RAW 264.7 NF-κB reporter cell line

RAW 264.7 NF-κB reporter cells, a modified murine macrophage cell line stably infected with lentivirus to express p65-EGFP fluorescent fusion proteins from the *RelA* (p65) promoter and destabilized mCherry from the *Tnf* promoter, were a kind gift from Dr. Iain Fraser (NIH, Bethesda, MD) and have been previously described[47]. These cells were maintained by serial passage in Dubecco's modified eagle medium (DMEM; Mediatech, Inc.) supplemented with 10% fetal bovine serum (FBS; Atlanta Biologicals, Norcross, GA), 1% Penicillin-Streptomycin (Sigma Aldrich), 1% L-glutamine (Invitrogen,

Carlsbad, CA), and 50 μg/mL gentamycin (Sigma Aldrich) in CytoOne T-75 cell culture flasks (USA-Scientific, Inc., Ocala, FL). Cells were cultured in a humidified incubator at 37°C with 5% CO_2.

2.2.2 Tissue culture procedures

Tissue culture was carried out in a class II biosafety cabinet using sterile technique. RAW cells were grown to ~80% confluence in culture flasks. To split cells, DMEM was removed from the flask by serological pipette, and the cells were rinsed with 10 mL warm sterile PBS, which was discarded. The cell monolayer was then lifted from the flask by cell scraper and washed with 5 mL sterile PBS. The cells in PBS were collected via serological pipette and placed in a 15 mL conical. The cells were then centrifuged at 400 × *g* (1355 rpm) for 5 minutes. PBS was removed and the cell pellet was resuspended in 5 mL warm DMEM. On average, RAW cells were split 1:4. This process constitutes one passage, and cells could be passaged up to twenty times before it became necessary to thaw new cells due to deteriorating cell growth rate.

2.2.3 Microscopy procedure

Day 1

The day before a microscope experiment, cells were plated in 35 mm glass bottom dishes (Cellvis, Mountain View, CA), which have a capacity of 2000 μL. Typically, two dishes were required for each experiment (a control and a treated plate). To plate cells, the initial steps in the procedure for splitting cells were followed (Section 2.2.2) to produce a single cell suspension. The viability of these cells was assessed via the Trypan blue (TB) dye exclusion method. A sample of cells was diluted 1:4 in TB (Sigma Aldrich), which selectively stains dead cells because live cells are impermeable to the dye. The cells were

then counted using a hemocytometer. Accurate hemocytometer counts require 60-200 cells/square, so a higher dilution factor was used if not enough cells were present in the initial dilution. The following formula was used to determine how to obtain the desired seeding density (1×10^5 cells/mL):

$$\mathbf{[A \times 10^4 \times D]x = (1 \times 10^5)(2000\ \mu L)}$$

…where A is the average number of cells/0.1 mL, D is the dilution factor, and x is the volume of cells in DMEM to be added to each dish. After allowing the cells to settle in the dish for ~6 hours, 100 units/mL murine interferon-gamma (IFNγ; Hoffmann-La Roche, Basel, Switzerland) was added to each plate.

Day 2

Before initiating each experiment, DMEM + IFNγ was removed from dishes and replaced by fresh warm DMEM. For GXM-treated cells, GXM was added at the indicated concentration one hour before adding LPS and imaging. All microscopy experiments were carried out using a Nikon T*i* Eclipse fluorescent microscope (Tokyo, Japan) equipped with a CoolSNAP MYO CCD camera (Photometrics, Tucson, AZ) and a complete microscope enclosure with a humidified chamber and CO_2 supply (InVivo Scientific, USA). For each plate, 8-10 fields were selected, and 100 ng/mL LPS was added to the cells. Immediately after adding LPS, cells were imaged for three hours at three-minute intervals. Appropriate filter sets were used to capture EGFP and mCherry fluorescence. Data were collected with NIS Elements AR software (Nikon).

2.2.4 Microscopy data analysis

Microscopy data were analyzed using FIJI, an open-source software for bioimaging analysis[48]. FIJI was used to measure fluorescence intensities by collecting mean and

integrated density values for user-specified regions of interest (ROIs). While mean is the average value of the pixels measured within a given ROI, integrated density is the sum of the values of those pixels. For EGFP fluorescence data, mean and integrated intensities were collected for nuclei and cytoplasm at each time point (61 time points/plate), and the nuclear(Nuc):cytoplasmic(Cyto) p65-EGFP ratios were calculated and compared. NF-κB was considered "active" when nuclear:cytoplasmic p65-EGFP fluorescence exceeded one. All data were processed to discount background signal.

2.3 Luminometry

Day 1

First, wildtype RAW 264.7 cells were transfected with ETF pNF-κB-Luc luciferase reporter plasmid DNA (Stratagene, La Jolla, CA) using Lipofectamine 3000 reagent (Thermo Scientific), a lipid-based transfection reagent. In brief, the cells were plated in 24-well plates. Lipofectamine 3000 reagent (5.25 μL) was diluted in 250 μL DMEM and agitated ~5 s. pNF-κB-Luc plasmid DNA (2 μg) was diluted in 250 μL DMEM, and 3 μL p3000 reagent (Thermo Scientific) was added. The diluted DNA was added to the Lipofectamine 3000 mixture and incubated at room temperature for 5 minutes. The mixture was then added to the cells (24 μL/well), and the cells were incubated overnight at 37°C in humidified conditions with 5% CO_2.

Day 2

The following day, cells were treated with GXM alone (200 μg/mL), LPS alone (100 ng/mL), or GXM + LPS. Control cells were treated with vehicle. There were three replicate wells for each treatment. One hour after treatment with GXM, 100 ng/mL LPS was added to the appropriate wells. Six hours later, luminometry was performed in the

following manner: the media was removed and 250 µL/well passive lysis buffer [0.025% (w/v) dithiothreitol (DTT), 1% (w/v) BSA, 25 mM Tris-phosphate, 1% Triton X-100, 15% (v/v) glycerol, 0.1 mM ethylenediaminetetraacetic acid (EDTA), 8 mM $MgCl_2$ prepared in diH_2O 5 µL/mL phenylmethanesulfonyl fluoride (PMSF)] was added to the cells. The plate was placed in a shaking incubator at 200 rpm, 37°C, for 15 minutes. Next, 10 µL of 25 mM adenosine triphosphate (ATP) was added to each well. The lysed contents of the wells were then transferred over to a 96-well plate as duplicate samples (100 µL/well) for a total of 6 wells per category. Sodium pyrophosphate (20 µL of 10 mM stock) was added to each well to stabilize the luciferase reaction, followed by 100 µL of Luciferin. Photonic emissions were immediately measured on the SpectraMax M5 microplate reader in relative light units (RLU). RLU readings were then averaged and normalized to the average control value.

2.4 Statistical analyses

Data were analyzed with GraphPad Prism (GraphPad Software, Inc., La Jolla, CA) using parametric or non-parametric analysis of variance (ANOVA). Based on Nuc:Cyto p65-EGFP fluorescence, three parameters were compared between LPS and GXM + LPS cells: maximum amplitude, time to maximum amplitude, and response duration (Figure 6). Time to maximum amplitude and response duration were compared using parametric ANOVA, while maximum amplitude was compared using Wilcoxon Signed Ranks test for non-parametric data. A p value of < 0.05 was considered significant for all comparisons.

3

RESULTS

3.1 Ultrafiltration yields more GXM than chemical precipitation.

3.1.1 Chemical precipitation: GXM + GalXM

Purified polysaccharides were weighed and concentrations were determined by ELISA and by calorimetric sugar assay (Table 1). By weight, 19.9 mg of GXM was isolated from Uge1, which is approximately four times the GXM yield of H99S. The GXM ELISA was performed in duplicate with H99S GXM + GalXM, H99S GXM, and Uge1 GXM. Only very small amounts of purified H99S- or Cap59-derived GalXM were obtained. Purified polysaccharide yields obtained following this method may have been low because multiple transfers of samples between conicals were required, and some conicals cracked, which probably resulted in loss of material. The LAL assay confirmed that Uge1-derived GXM purified by chemical precipitation was negative for endotoxin/LPS contamination (< 0.017 EU/mL).

3.1.2 Ultrafiltration: GXM

Considerably more GXM was obtained by ultrafiltration than by chemical precipitation; 88.4 mg of GXM (by weight) was isolated from Uge1 supernatant using this method. The GXM ELISA reported concentrations of 3.97 mg/mL and 3.16 mg/mL (Table 1). Because the LAL assay demonstrated contaminating LPS in these samples (> 0.3 EU/mL), the calorimetric sugar assay was not performed since it would detect both LPS and GXM.

3.2 GXM suppresses LPS-induced nuclear translocation of p65-EGFP in murine macrophages.

The effects of GXM on NF-κB signaling dynamics were investigated using RAW 264.7 NF-κB reporter cells treated for 1 hour with GXM followed by LPS stimulation. All experiments employed LPS-free Uge1 GXM obtained by chemical precipitation (Table 2). First, the appropriate GXM dose was determined by trial experiments (summarized in Table 2). Literature sources indicated standard experimental GXM doses ranged from 50 to 200 μg/mL, and RAW 264.7 NF-κB reporter cells were treated with LPS alone or with GXM at a concentration of 50, 100, or 200 μg/mL (Figure 7). In three initial microscopy experiments, macrophages became dehydrated and shriveled, possibly as a consequence of CTAB and NaCl contamination of the GXM preps. To remove these contaminants, GXM preps were dialyzed in diH_2O, precipitated in ethanol, and washed with 2% acetic acid in ethanol, 90% ethanol, and absolute ethanol and then processed to remove LPS again using the PMB column (Figure 3). LPS-stimulated translocation of p65 (Nuc:Cyto p65-EGFP) was greatly reduced in cells pre-treated with 200 μg/mL GXM. However, 100 μg/mL only slightly suppressed p65 translocation and no effect was observed when GXM concentrations were decreased to 50 μg/mL (Figure 7). Based on these data, all subsequent experiments were performed using 200 μg/mL GXM.

In three independent biological repeats, RAW 264.7 NF-κB reporter cells were treated with 200 μg/mL GXM for 1 hour followed by LPS (GXM + LPS) or LPS alone (LPS; Figure 8). A Wilcoxon Signed Ranks test demonstrated maximum amplitude was significantly attenuated in GXM + LPS cells compared to LPS cells, Z = -8.3875, p < 0.0001. Time to maximum amplitude was also significantly decreased as reported by

ANOVA, $F(1) = 17.0781$, $p < 0.0001$. A trend toward shorter response duration in GXM + LPS cells was observed, $F(1) = 2.75$, $p = 0.09$.

3.3 GXM does not alter NF-κB-dependent transcription in murine macrophages.

A luciferase assay was performed to determine whether GXM-dependent suppression of p65 nuclear translocation affects NF-κB promoter transactivation. RAW 264.7 cells transfected with pNF-κB-Luc (plasmid DNA containing the firefly luciferase gene under control of a synthetic NF-κB regulated promoter composed of five tandem consensus κB sites) were treated with vehicle (Control), 200 μg/mL GXM (GXM), 100 ng/mL LPS (LPS), or 200 μg/mL GXM for 1 hour prior to LPS (GXM + LPS). Cells were incubated with LPS for a further 6 h. In order to assay for luciferase expression, an indirect measure of NF-κB-regulated gene expression, the cells were lysed and luminometry was performed. Basal and LPS-induced luciferase expression was attenuated slightly by GXM treatment, but this did not reach statistical significance in either case (Figure 9).

4

DISCUSSION

4.1 Significance

This is the first investigation of GXM-dependent canonical NF-κB signaling using live cell imaging, which allowed detailed observation of NF-κB signaling dynamics at high temporal resolution in individual cells. In RAW 264.7 NF-κB reporter cells, GXM significantly decreased maximum Nuc:Cyto p65-EGFP response amplitude and time to achieve maximum amplitude. These findings allow comparisons between the effects of GXM and whole intra- and extracellular *Cn* on NF-κB signaling dynamics. The effects of extracellular *Cn* on NF-κB activity have been studied extensively[21,26,37,39]. However, the precise mechanisms by which *Cn* modulates NF-κB activity have yet to be elucidated, and to our knowledge no study has investigated the effects of internalized *Cn* on NF-κB signaling. Experiments performed by James Hayes (Nelson and McClelland labs, MTSU) have demonstrated intracellular *Cn* alters NF-κB signaling dynamics differently than extracellular *Cn* or GXM[49]. Like GXM, whole intracellular *Cn* infection delays time to maximum Nuc:Cyto p65-EGFP amplitude in RAW 264.7 NF-κB reporter cells. However, intracellular *Cn* significantly increases maximum amplitude achieved and prolongs response duration. Thus, *Cn* modulates NF-κB by distinct mechanisms during the intracellular and extracellular phases of *Cn* infections in macrophages.

GXM polymers are variable in 3D structure and molecular mass[50], which could have important implications for purification methods. Although precipitation with CTAB is widely used to isolate GXM, it is difficult to remove from the final product. Furthermore, it is unclear whether contamination with CTAB could alter GXM structure

or its biological effects[51]. Nimrichter *et al* demonstrated the utility of ultrafiltration for GXM purification[42]. GXM purified by ultrafiltration was analyzed by gas chromatography, mass spectrometry, and nuclear magnetic resonance, which confirmed the presence of GXM building blocks with minimal or no GalXM contamination. Molecular mass of GXM prepared by this method was nine-fold smaller than molecular mass of GXM precipitated by CTAB. According to Albuquerque *et al*, GXM molecular mass does not affect uptake by murine macrophages[52]. However, different molecular masses elicit different cytokine profiles in macrophages, and macrophages stimulated with GXM samples comprised of the full range of molecular masses exhibit the most efficient cytokine output. Further investigation is needed to define the differences between GXM isolated by ultrafiltration and CTAB precipitation.

4.2 Limitations

The concentrations given by the GXM ELISA and the calorimetric sugar assay, which detect different characteristics of GXM, did not agree with the measurements of GXM weight. Because mAb 18b7 may only bind certain types of GXM polymers[51] and because the ELISA error rate is 100%, we elected to use weight measurements when planning experiments. Additionally, we did not have a reliable validated method for determining which cells in our system endocytosed GXM. However, I am confident this did not affect our results because (i) an effect was observed (Figure 8) and (ii) prior studies[39,52] have demonstrated GXM is taken up by 60-70% of RAW 264.7 cells using GXM bound by fluorescently-labeled 18B7.

4.3 Future directions

Profound suppression of NF-κB activation by GXM raises the question of whether targets of NF-κB, such as TNFα and inducible nitric oxide synthase (iNOS), are reduced in this experimental model of *Cn* infection in macrophages. Studies using endpoint assays have shown TNFα is suppressed in RAW 264.7 cells treated with GXM[26,37,39]. Longer microscopy experiments will be conducted in which GXM-treated cells are imaged for a minimum of ten hours, and TNFα production will be compared between LPS and GXM + LPS cells. iNOS production is a hallmark of macrophage 'activation,' a heightened anti-microbial state that is essential for macrophage killing of pathogens such as *Cn*[53]. The amount of iNOS present in LPS-stimulated RAW 264.7 cells treated with or without GXM will be visualized and quantified by immunofluorescent staining or by the production of new RAW 264.7 reporter cell lines incorporating fluorescent reporters of iNOS gene transactivation. In addition, the luciferase assay could be repeated to see if additional experiments reveal significant attenuation of NF-κB transactivation by GXM using this technique. RAW 264.7 cells infected with *Cn*[21] or exposed to GXM[54] have exhibited increased NF-κB transactivation measured by NF-κB-luciferase assay in other studies.

No Uge1 GXM prepared by chemical precipitation remained at the completion of this project. Additional investigations using GXM will rely on the samples purified by ultrafiltration. After LPS is removed from the samples, the GXM ELISA and the calorimetric sugar assay will be performed to determine the GXM concentration. Before other studies proceed, the experiment in which RAW 264.7 NF-κB reporter cells were

treated with 200 μg/mL GXM prior to LPS stimulation will be repeated and analyzed to determine if the results are replicable using GXM prepared by ultrafiltration.

Polysaccharide purification was a new technique to both the Nelson and McClelland labs, and a significant period of trial and error was required to develop the methodologies. Thus, non-canonical NF-κB signaling dynamics were not investigated, nor was GalXM purified. Little is currently known about the immunological properties of GalXM. Future projects will include purifying and validating GalXM and conducting live cell microscopy experiments with GalXM to determine its effects on NF-κB signaling dynamics in RAW 264.7 cells.

4.4 Conclusions

In closing, this study was the first to demonstrate GXM-dependent suppression of NF-κB signaling in macrophages using a live cell microscopy approach. This project was an essential component of an ongoing research effort by the Nelson and McClelland laboratories to investigate the mechanisms by which intracellular *Cn* modulates NF-κB signaling. In addition, methodologies for purifying cryptococcal polysaccharides were developed, and a large quantity of purified GXM was obtained for future studies. When coupled with studies involving intracellular *Cn*, the results of this project will yield valuable insights into the mechanisms by which *Cn* subverts the host immune response.

References

1. Lin, Xiaorong and Joseph Heitman. The biology of the Cryptococcus neoformans species complex. *Annu Rev Microbiol.* 2006;60:69-105.
2. Srikata D, Santiago-Tirado FH, Doering TL. Cryptococcus neoformans: historical curiosity to modern pathogen. *Yeast.* 2014;31(2):47–60.
3. Saag MS, Graybill RJ, Larsen RA, Pappas PG, Perfect JR, Powderly WG, Sobel JD, Dismukes WE. Practice guidelines for the management of cryptococcal disease. Infectious Diseases Society of America. *Clin Infect Dis.* 2000 Apr;30(4):710-8.
4. McClelland EE, Bernhardt P, Casadevall A. Estimating the Relative Contributions of Virulence Factors for Pathogenic Microbes. *Infect Immun.* 2006;74(3):1500-1504.
5. Doering TL. How does Cryptococcus get its coat? *Trends Microbiol.* 2000;8:547–553.
6. Zargoza O, Rodrigues ML, De Jesus M, Frases S, Dadachova E, Casadevall A. The capsule of the fungal pathogen Cryptococcus neoformans. *Adv Appl Microbiol*. 2009;68:133–216.
7. Eng, R. H., E. Bishburg, S. M. Smith, R. Kapila. 1986. Cryptococcal infections in patients with acquired immune deficiency syndrome. *Am. J. Med.* 81:19
8. Lee, S. C., A. Casadevall, D. W. Dickson. 1996. Immunohistochemical localization of capsular polysaccharide antigen in the central nervous system cells in cryptococcal meningoencephalitis. *Am. J. Pathol.* 148:1267
9. Lee, S. C., A. Casadevall. 1996. Polysaccharide antigen in brain tissue of AIDS patients with cryptococcal meningitis. *Clin. Infect. Dis.* 23:194
10. Mitchell, Thomas G. and John R. Perfect. Cryptococcosis in the era of AIDS--100 years after the discovery of Cryptococcus neoformans. *Clin Microbiol Rev.* 1995;8(4):515-548.
11. Del Valle, Luis and Sergio Piña-Oviedo. HIV disorders of the brain: pathology and pathogenesis. *Front Biosci*. 2006;11:718-732.
12. Sanfelice, F. Contributo alla morfologia e biologia dei si nei di alcuni frutti. *Ann. Igien*. 1894;4:463–495.
13. Busse O. Ueber parasitare zelleinschlusse und ihre zuchtung. *Zentralbl. Bakteriol*. 1894;16:175–180.
14. Buschke A. Ueber eine durch Coccidien Hervergerufene Krankheit des menschen. *Dtsch. Med. Wochenschr*. 1895;21(3):14.
15. Von Hansemann, D. U¨ber eine bisher nicht beobachtete Gehirner Krankung durch Hefen. *Verh. Dtsch. Ges. Pathol.* 1905;9:21–24.
16. Steenbergen, JN, Casadevall A. The origin and maintenance of virulence for the human pathogenic fungus *Cryptococcus neoformans. Microbes and Infection.* 2003;5(7):667-675.
17. Coelho C, Bocca AL, Casadevall A. The intracellular life of Cryptococcus neoformans. *Annu Rev Pathol.* 2014;9:219-38.
18. Chang ZL, Netski D, Thorkildson P, Kozel TR. Binding and Internalization of Glucuronoxylomannan, the Major Capsular Polysaccharide of *Cryptococcus neoformans*, by Murine Peritoneal Macrophages. *Infection and Immunity*. 2006;74(1):144-151. doi:10.1128/IAI.74.1.144-151.2006.

19. Bader T, Nettesheim P. Tumor necrosis factor-alpha modulates the expression of its p60 receptor and several cytokines in rat tracheal epithelial cells. *J Immunol.* 1996 Oct 1;157(7):3089-96.
20. Parameswaran N, Patial S. Tumor necrosis factor-α signaling in macrophages. *Crit Rev Eukaryot Gene Expr.* 2010;20(2):87-103.
21. Ben-Abdallah M, Sturny-Leclere A, Ave P, Louise A, Moyrand Frederique, Weih F, Janbon G, Memet S. Fungal-Induced Cell Cycle Impairment, Chromosome Instability and Apoptosis via Differential Activation of NF-kB. *PLoS Pathog.* 2012;8(3).
22. Goldman DL, Lee SC, Mednick AJ, Montella L, Casadevall A. Persistent*Cryptococcus neoformans* Pulmonary Infection in the Rat Is Associated with Intracellular Parasitism, Decreased Inducible Nitric Oxide Synthase Expression, and Altered Antibody Responsiveness to Cryptococcal Polysaccharide. Kozel TR, ed. *Infection and Immunity*. 2000;68(2):832-838.
23. Grinsell M, Weinhold LC, Cutler JE, Han Y, Kozel TR. In vivo clearance of glucuronoxylomannan, the major capsular polysaccharide of Cryptococcus neoformans: a critical role for tissue macrophages. *J Infect Dis*. 2001;184:479–487.
24. Alvarez M, Casadevall A. Phagosome Extrusion and Host-Cell Survival after Cryptococcus neoformans Phagocytosis by Macrophages. *Curr Biol*. 2006;16(21):2151-2165.
25. McClelland EE, Casadevall A and Eisenman HC. Pathogenesis of *Cryptococcus neoformans* in New Insights in Fungal Pathogenicity. 2007. Editor: Kevin Kavanagh, Springer.
26. Shoham S, Huang C, Chen JM, Golenbock DT, Levitz SM. Toll-like receptor 4 mediates intracellular signaling without TNF-alpha release in response to Cryptococcus neoformans polysaccharide capsule. *J Immunol*. 2001;166(7):4620-4626.
27. Vecchiarelli A, Pericolini E, Gabrielli E, Kenno S, Perito S, Cenci E, Monari C. Elucidating the immunological function of the Cryptococcus neoformans capsule. *Future Microbiol*. 2013;8(9):1107-1116.
28. Gerondakis S, Grumont R, Gugasyan R, Wong L, Isomura I, Ho W, Banerjee A. Unraveling the complexities of the NF-kB pathway using mouse knockout models. *Oncogene.* 2006;25:6781-6799.
29. Janssens S, Tschopp J. Signals from within: the DNA-damage-induced NF-kappaB response. *Cell Death Differ*. 2006 May;13(5):773-84.
30. Pahl HL (1999) Activators and target genes of Rel/NF-kappaB transcription factors. *Oncogene* 18: 6853–6866
31. Perfect JR, Dismukes WE, Dromer F, Goldman DL, Graybill JR, Hamill RJ, Harrison TS, Larsen RA, Lortholary O, Nguyen MH, Pappas PG, Powderly WG, Singh N, Sobel JD, Sorrell TC. Clinical practice guidelines for the management of cryptococcal disease: 2010 update by the Infectious Diseases Society of America. *Clin Infect Dis*. 2010 Feb 1;50(3):291-322.
32. Jackson A, Hosseinipour MC. Management of cryptococcal meningitis in sub-saharan Africa. *Curr HIV/AIDS Rep*. 2010;7(3):134-42.

33. Perfect JR, Cox GM. Drug resistance in Cryptococcus neoformans. *Drug Resist Updat*. 1999;2(4):259-269.
34. Bii, C. C., Makimura, K., Abe, S., Taguchi, H., Mugasia, O. M., Revathi, G., Wamae, N. C. and Kamiya, S. Antifungal drug susceptibility of *Cryptococcus neoformans* from clinical sources in Nairobi, Kenya. *Mycoses*. 2007;50: 25–30.
35. Vecchiarelli A, Retini C, Monari C, Tascini C, Bistoni F, Kozel TR. Purified capsular polysaccharide of *Cryptoccocus neoformans* induces interleukin-10 secretion by human monocytes. *Infect. Immun.* 64(7), 2846–2849 (1996).
36. Monari C, Kozel TR, Paganelli F, Pericolini E, Perito S, Bistoni F, Casadevall A, Vecchiarelli A. Microbial immune suppression mediated by direct engagement of inhibitory Fc receptor. *Immunol*. 177(10), 6842–6851 (2006).
37. Piccioni M, Monari C, Kenno S, Pericolini E, Gabrielli E, Pietrella D, Perito S, Bistoni F, Kozel TR, Vecchiarelli A. A purified capsular polysaccharide markedly inhibits inflammatory response during endotoxic shock. *Infect Immun*. 2013;81(1):90-8.
38. Park BS, Lee JO Recognition of lipopolysaccharide pattern by TLR4 complexes. *Experimental & Molecular Medicine* 2013;45, e66; doi:10.1038/emm.2013.97
39. Monari C, Pericolini E, Bistoni G, Casadevall A, Kozel TR, Vecchiarelli A. Cryptococcus neoformans capsular glucuronoxylomannan induces expression of fas ligand in macrophages. *J Immunol*. 2005 Mar 15;174(6):3461-8.
40. Cherniak R, Reiss E, Turner SH. A Galactoxylomannan Antigen of Cryptococcus neoformans, serotype A. *Carbohydrate Research*, 1982;103:239-250.
41. Villena SN, Pinheiro RO, Pinheiro CS, Nunes MP, Takiya CM, DosReis GA, Previato JO, Mendonca-Previato L, Freire-de-Lima CG. Capsular polysaccharides galactoxylomannan and glucuronoxylomannan from Cryptococcus neoformans induce macrophage apoptosis mediated by Fas ligand. *Cell Microbiol*. 2008;10(6)1274-85.
42. Nimrichter L, Frases S, Cinelli LP, Viana NB, Nakouzi A, Travassos LR, Casadevall A, Rodrigues ML. Self-Aggregation of *Cryptococcus neoformans* Capsular Glucuronoxylomannan Is Dependent on Divalent Cations. *Eukaryotic Cell*. 2007;6(8):1400-1410.
43. Moore RA, Bates NC, Hancock RE. Interaction of polycationic antibiotics with Pseudomonas aeruginosa lipopolysaccharide and lipid A studied by using dansyl-polymyxin. *Antimicrobial Agents and Chemotherapy*. 1986;29(3):496-500.
44. Casadevall A, Cleare W, Feldmesser M, Glatman-Freedman A, Goldman DL, Kozel TR, Lendvai N, Mukherjee J, Pirofski LA, Rivera J, Rosas AL, Scharff MD, Valadon P, Westin K, Zhong Z. Characterization of a Murine Monoclonal Antibody to *Cryptococcus neoformans* Polysaccharide That Is a Candidate for Human Therapeutic Studies. *Antimicrobial Agents and Chemotherapy*. 1998;42(6):1437-1446.
45. Mukherjee J, Casadevall A, Scharff MD. Molecular characterization of the humoral responses to Cryptococcus neoformans infection and glucuronoxylomannan-tetanus toxoid conjugate immunization. *The Journal of Experimental Medicine*. 1993;177(4):1105-1116.

46. Dubois M, Gilles K, Hamilton JK, Rebers PA, Smith F. A calorimetric method for the determination of sugars. *Nature*. 1951;168(4265)167.
47. Sung MH, Li N, Lao Q, Gottschalk RA, Hager GL, Fraser IDC. Switching of the relative dominance between feedback mechanisms in lipopolysaccharide-induced nf-κb signaling. *Science signaling* 2014; 7(308):ra6
48. Schindelin J, Arganda-Carreras I, Frise E, Kaynig V, Longair M, Pietzsch T, Preibisch S, Rueden C, Saalfeld S, Schmid B, Tinevez JY, White DJ, Hartenstein V, Eliceiri K, Tomancak P, Cardona A. Fiji - an Open Source platform for biological image analysis. *Nature methods*. 2012;9(7): 676-82.
49. Hayes JB, Heusinkveld LE, Ding W, Leander RN, McClelland EE, Nelson DE. Modulation of macrophage inflammatory NF-κB signaling by intracellular Cryptococcus neoformans. (submitted to *Journal of Biological Chemistry*).
50. Rodrigues ML, Nimrichter L, Cordero RJB, Casadevall A. Fungal Polysaccharides: Biological Activity Beyond the Usual Structural Properties.*Frontiers in Microbiology*. 2011;2:171.
51. Rodrigues ML, Fonseca FL, Frases S, Casadevall A, Nimrichter L. The still obscure attributes of cryptococcal glucuronoxylomannan. *Medical mycology*. 2009;47(8):783-788. doi:10.3109/13693780902788621.
52. Albuquerque PC, Fonseca FL, Dutra FF, Bozza MT, Frases S, Casadevall A, Rodrigues ML. *Cryptococcus neoformans* glucuronoxylomannan fractions of different molecular masses are functionally distinct. *Future microbiology*. 2014;9(2):147-161.
53. Winston BW, Krein PM, Mowat C, Huang Y. Cytokine-induced macrophage differentiation: a tale of 2 genes. *Clin Invest Med*. 1999;22(6):236-55.
54. Fonseca FL, Nohara LL, Cordero RJB, Frases S, Casadevall A, Almeida IC, Nimrichter L, Rodrigues ML. Immunomodulatory Effects of Serotype B Glucuronoxylomannan from Cryptococcus gattii Correlate with Polysaccharide Diameter. *Infection and Immunity*. 2010;78(9):3861-3870.
55. Wu P, Imai M. Novel Biopolymer Composite Membrane Involved with Selective Mass Transfer and Excellent Water Permeability. In: Ning YL, ed. *Advancing Desalination*. Rijeka, Croatia: InTech; 2012.

Appendix

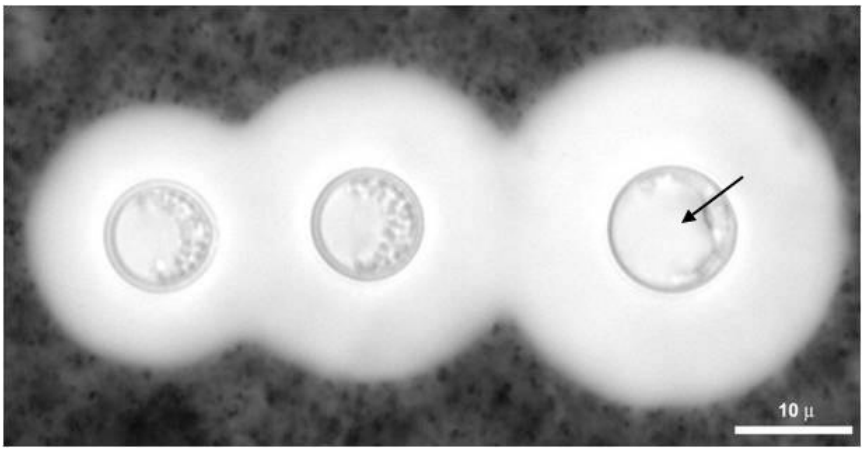

Figure 1: ***Cryptococcus neoformans.*** *Cn* is protected by a dense capsule composed primarily of two polysaccharides, glucuronoxylomannan and galactoxylomannan. In the image above, whole *Cn* were stained with India Ink and imaged via light microscopy. The capsule appears opaque white, and an arrow indicates the cell body. (Courtesy of Dr. McClelland).

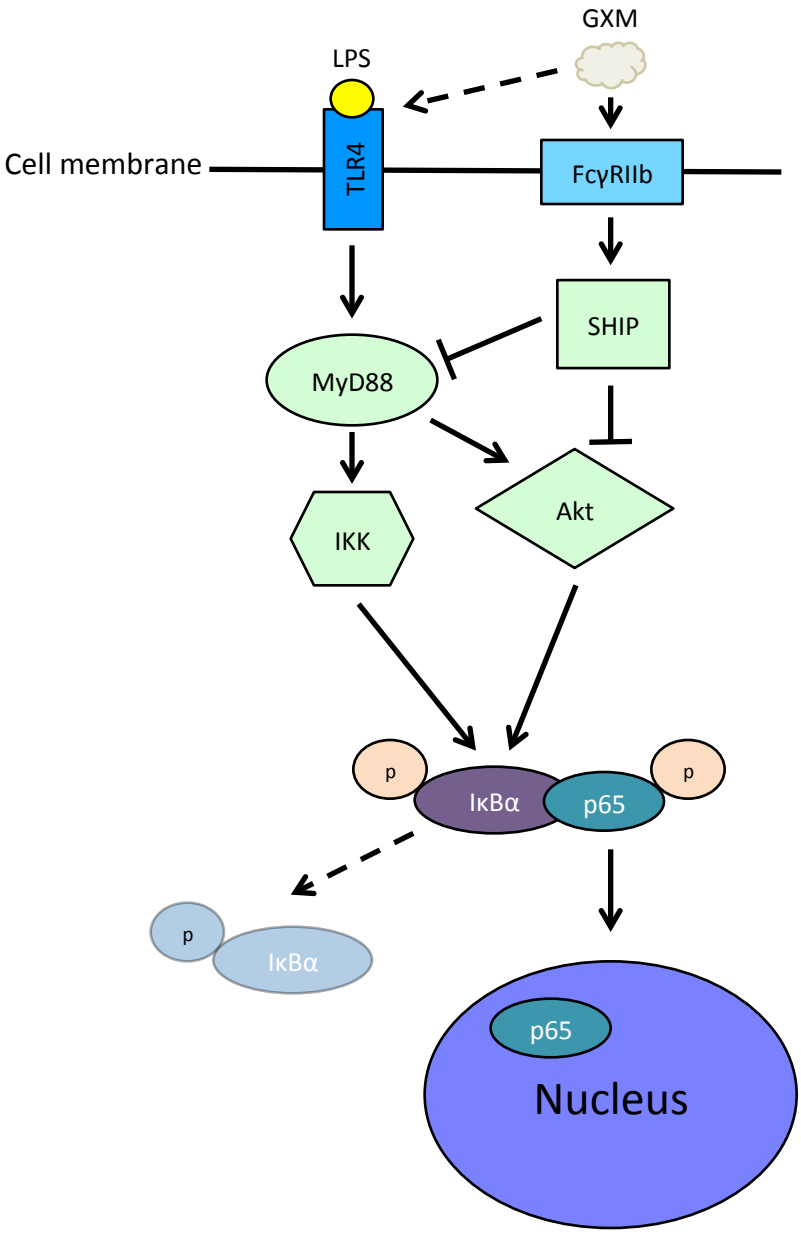

Figure 2: Proposed mechanism by which GXM inhibits LPS-induced NF-κB signaling. Extracellular GXM is recognized by macrophage receptors TLR4 and FcγRIIb. TLR4 is the primary receptor for LPS, a potent activator of NF-κB. LPS induces MyD88 recruitment, which leads to activation of IKK and Akt. NF-κB activation is preceded by simultaneous phosphorylation of IκBα and p65. Phospho-IκBα is subsequently degraded and p65 translocates to the nucleus. Meanwhile, binding of FcγRIIb by GXM induces SHIP activation, which inhibits MyD88 recruitment and Akt activation, thus inhibiting TLR4-directed p65 translocation. Adapted from Piccioni *et al*[37].

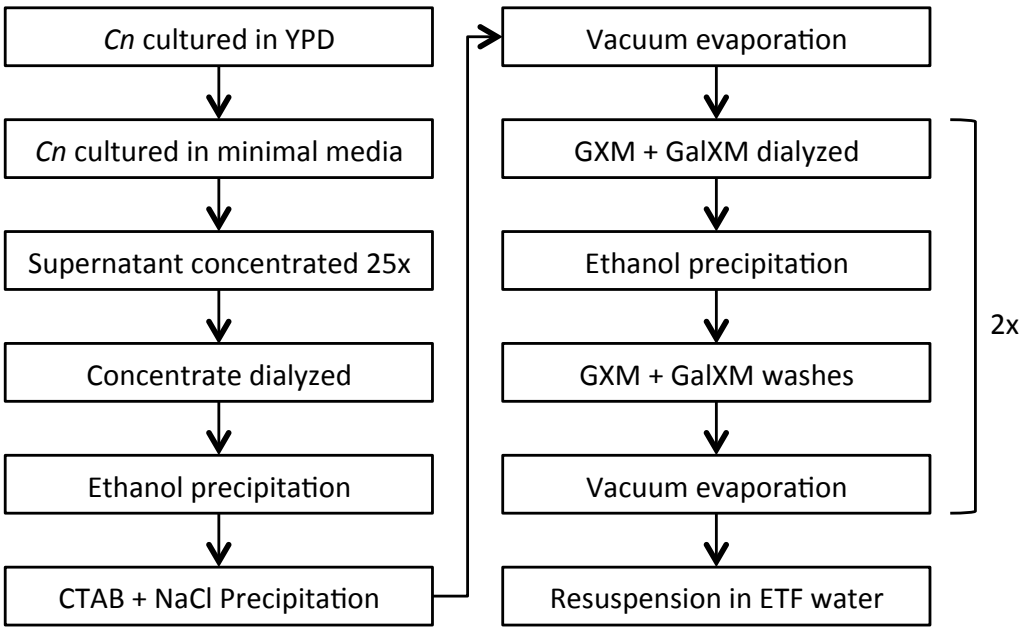

Figure 3: Chemical precipitation of GXM and GalXM from *Cn* culture supernatant. In this twelve-step process, *Cn* culture supernatant was first concentrated and dialyzed against diH_2O. Polysaccharides were then purified by precipitation with ethanol, CTAB, and NaCl. Samples were dried by vacuum concentration, and dialysis, ethanol precipitation, washes, and vacuum evaporation were repeated twice more. Finally, the samples were resuspended in ETF water.

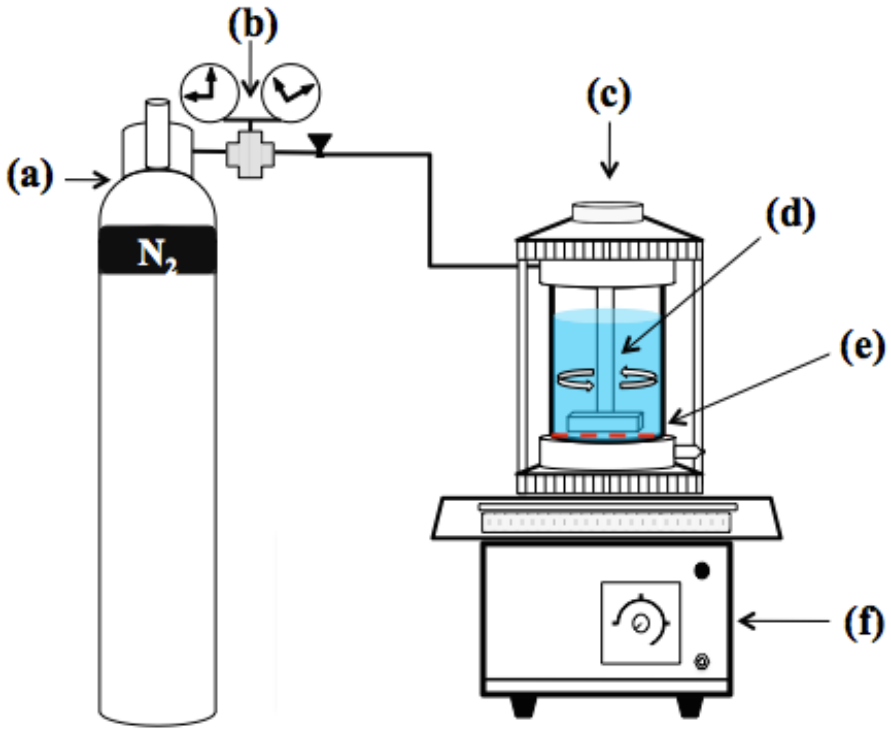

Figure 4: Stirred ultrafiltration configuration. The filtration cell (c) sits atop a stir plate (f), which rotates the stir bar (d). Pressurized nitrogen gas (a) forces the supernatant through the membrane (e), which collects polysaccharide. A regulator (b) controls gas pressure. After passing through the membrane, excess supernatant is collected in a beaker (not shown). Adapted from Wu and Imai[54].

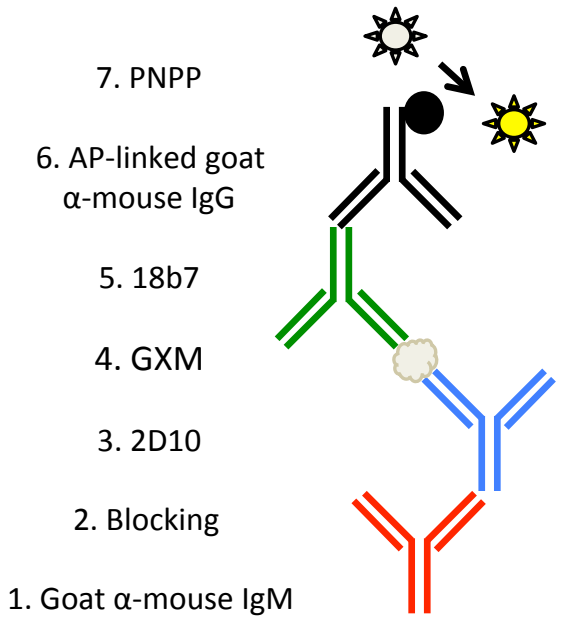

Figure 5: Sandwich ELISA for GXM. GXM was verified and quantified by a seven-step sandwich ELISA. Goat anti-mouse mAb IgM was added to coat the bottom of the plate. The plate was blocked overnight with 1% BSA (not represented) to prevent nonspecific binding of ELISA components and then washed with TBS/T. mAb 2D10 was added followed by GXM and the washes were repeated. The plate was incubated with mAb 18b7 and washed. AP-linked goat anti-mouse mAb IgG and PNPP, an AP substrate producing a yellow product, were added and the absorbance at 405 nm was read.

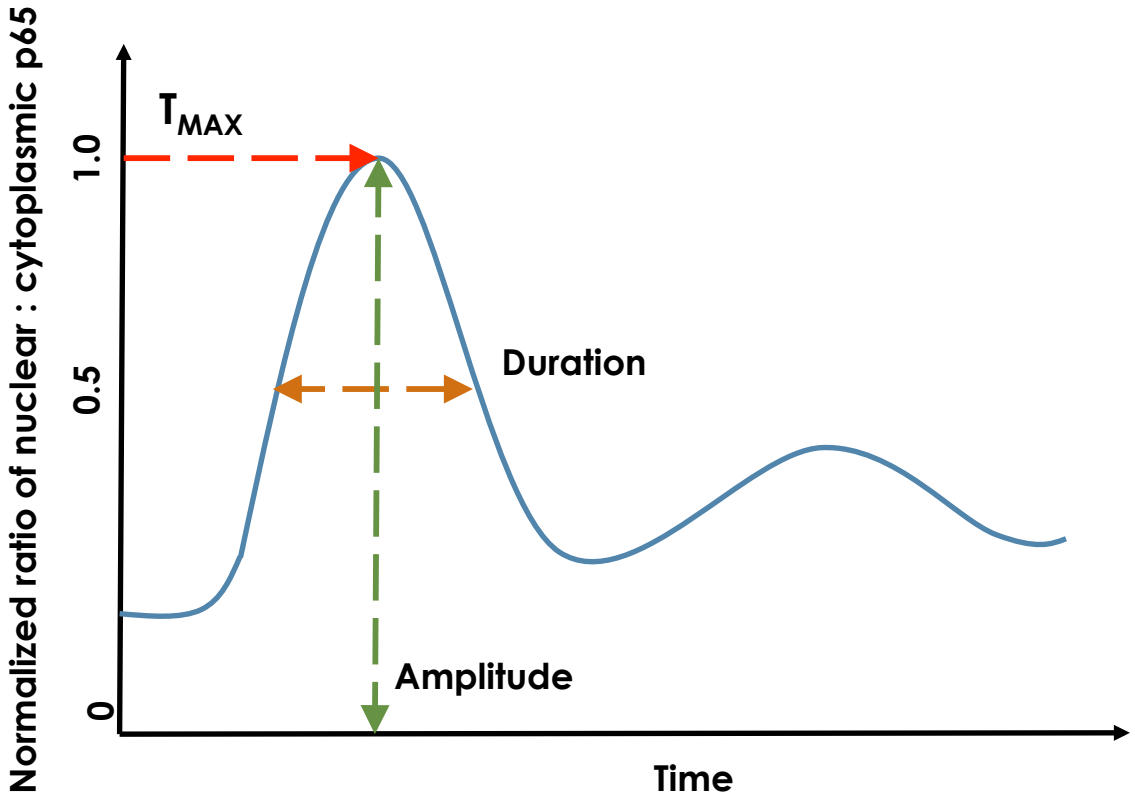

Figure 6: Parameters compared between RAW 264.7 NF-κB reporter cells treated with and without GXM. After calculating Nuc:Cyto p65-EGFP fluorescence, three parameters were compared between LPS and GXM + LPS cells. Maximum amplitude is the highest amplitude achieved prior to t = 60 minutes. Time to maximum amplitude (T_{max}) is time in minutes between t = 0 and maximum amplitude. Response duration is measured in minutes between Nuc:Cyto > 0.5 and Nuc:Cyto < 0.5. (Courtesy of James Hayes, MTSU)

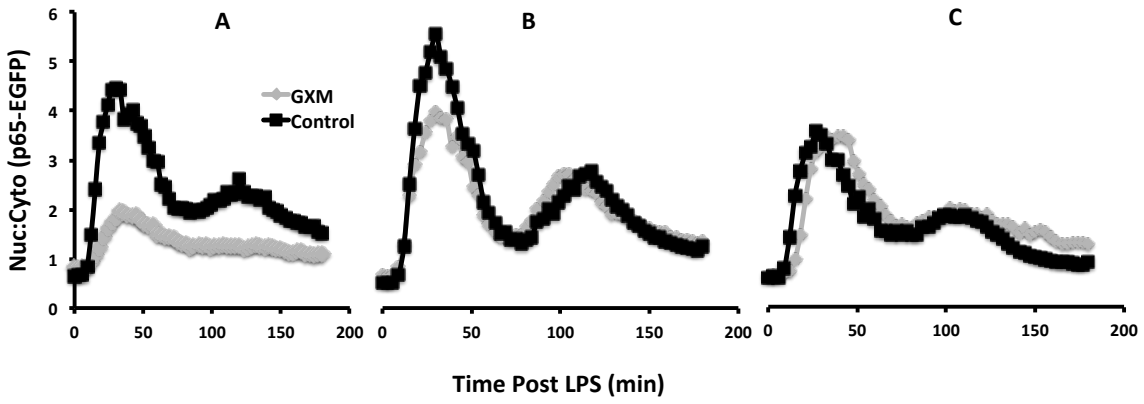

Figure 7: Effect of varying concentrations of GXM on LPS-induced nuclear translocation of p65. RAW 264.7 NF-κB reporter cells were treated with LPS alone or (A) 200, (B) 100, or (C) 50 μg/mL GXM for 1 hour prior to LPS. Cells were imaged every 3 min over a 180 min period immediately following LPS treatment. The nuclear:cytoplasmic ratio of p65-EGFP fluorescence was quantified for individual cells. Average population data from a single representative experiment is shown. n > 35 cells for each condition.

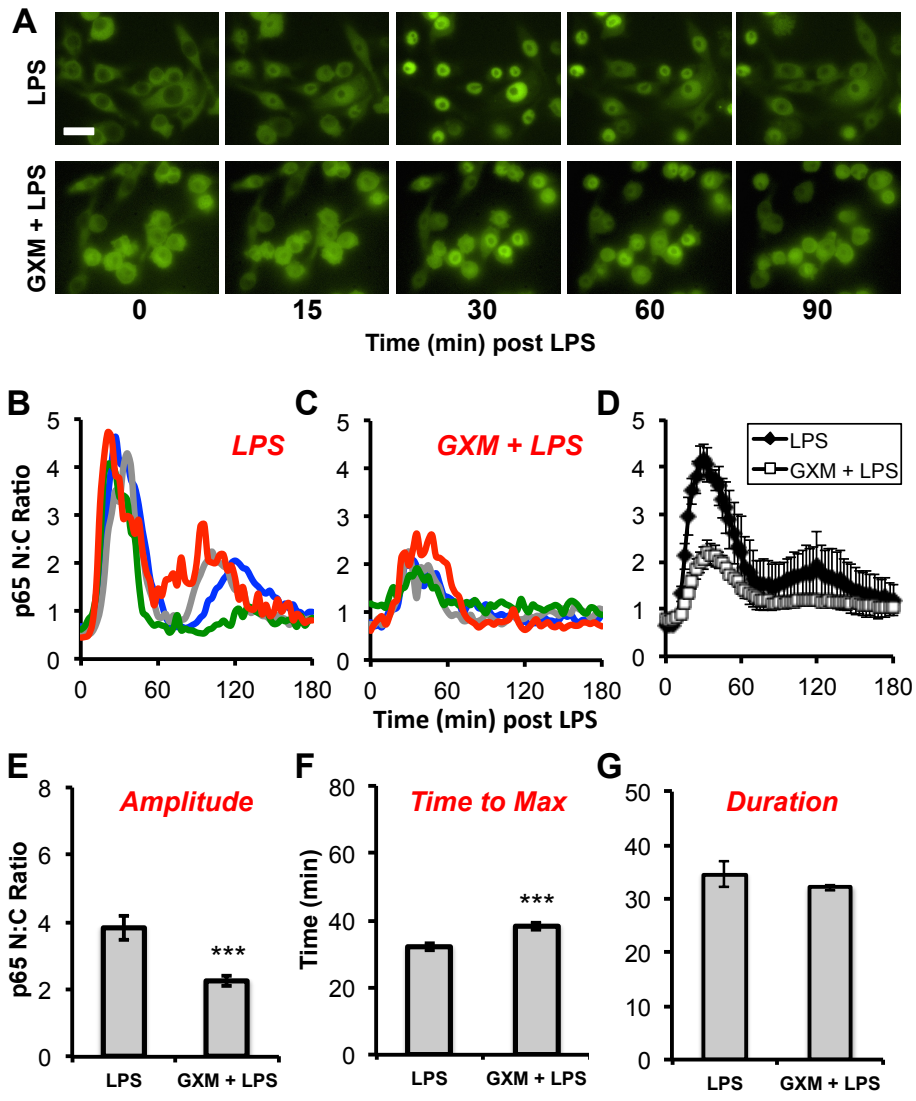

Figure 8: Uge1-derived GXM suppresses p65 nuclear translocation in RAW 264.7 cells stimulated with LPS. RAW 264.7 NF-κB reporter cells were treated with 200 μg/mL GXM for 1 hour followed by LPS (GXM + LPS) or LPS alone (LPS). (A) Time course fluorescence microscopy images of p65-EGFP (green) localization in RAW 264.7 are displayed. Scale bar represents 20 μm. (B-D) Single cell trajectories of Nuclear:Cytoplasmic p65-EGFP fluorescence post LPS (B) without and (C) with GXM pretreatment for 4 representative cells and (D) the population average demonstrate attenuated LPS-induced p65 translocation in response to GXM pre-treatment. Average (E) maximum amplitude, (F) time to achieve maximum amplitude, and (G) response duration are displayed. Error is represented as the SE. Statistical significance is indicated as follows, ***$p < 0.001$ (ANOVA). Data from > 100 cells were collected per condition across 3 independent biological repeats. In F, data were pooled from two experiments, n > 70 cells per condition.

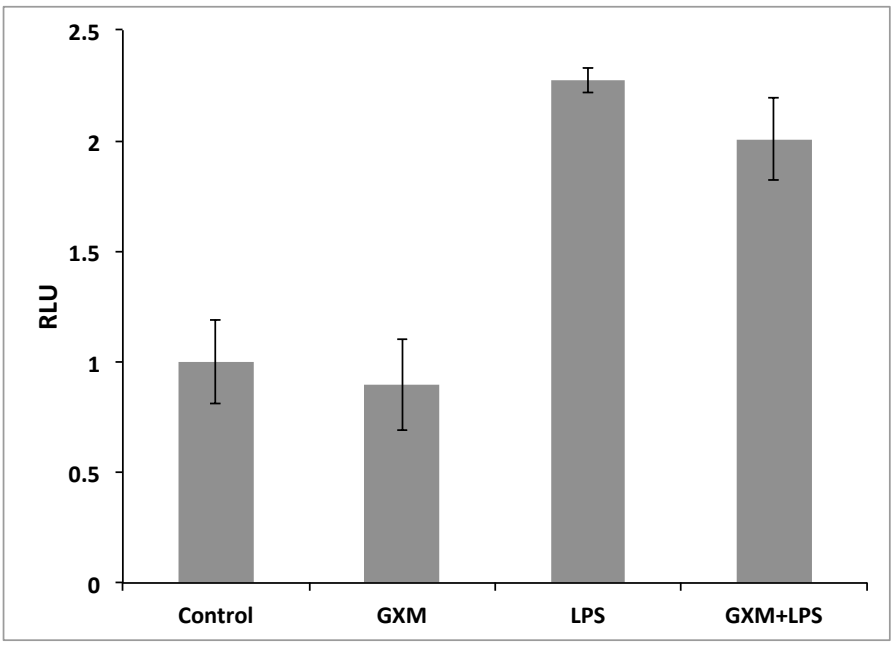

Figure 9: GXM does not suppress NF-κB-dependent transcription. RAW 264.7 cells transfected with pNF-κB-Luc were treated with vehicle (Control) or 200 μg/mL GXM (GXM) for 1 hour prior to LPS (GXM + LPS). Cells were lysed in passive lysis buffer and assayed for luciferase expression by luminometry six hours post LPS. Data are average values normalized to the average control value in RLU. Error is represented as the SE.

Table 1

Cryptococcal polysaccharide yields

Method	Sample	Weight (mg)	ELISA	Sugar Assay (μg/mL)
Chemical precipitation	Uge1 GXM	19.9	12.696 mg/mL	2.6099
	H99S GXM	4.7	668.261 ng/mL	-
	H99S GXM + GalXM	3.4	1.794 ng/mL	-
Ultrafiltration	Uge1 GXM	88.4	3.97 mg/mL 3.16 mg/mL	-

Polysaccharide samples purified by chemical precipitation were weighed, and concentrations were determined by GXM ELISA and by a calorimetric sugar assay. Uge1 GXM obtained by ultrafiltration was weighed and concentration was measured by GXM ELISA. Representative data from ELISA experiments are displayed. Concentrations from two samples of Uge1 reported by ELISA are displayed.

Table 2

Fluorescence microscopy experiments

Replicates	GXM (μg/mL)	LPS (ng/mL)	Time	Data Usable
3	200	100	3 (3)	3 reps
1	1000	100	3 (3)	-
2	100	100	3 (3)	2 reps
1	60	-	1 (3)	-
2	50	100	3 (3)	1 reps
1	200	100	10 (6)	-

The number of replicates for each GXM dose (200, 100, 50 μg/mL) is shown. Time is represented as "length of experiment in hours (minutes between each time point)". In all experiments, 100 ng/mL LPS was added to stimulate nuclear translocation of p65-EGFP.